Research on synergistic effect and bearing capacity of solar composite roof panel

Junwu Xia[1,2], Renqing Li[1], Peng Gong[1] and Linli Yu[1]

[1]State Key Laboratory for Geomechanics and Deep Underground Engineering, China University of Mining and Technology, Xuzhou 221116, China

[2]Jiangsu Collaborative Innovation Center for Building Energy Saving and Construct Technology, Xuzhou 221116，China

E-mail: 02120567@cumt.edu.cn

Abstract. Taking the two new connection forms of PV (photovoltaic) panels and sloping roof — "external form" and "embedded form" designed in this paper as the research objects, the bearing performance of PV panels have been studied by static loading test. The deflection and strain characteristics of PV panels under two kinds of connection forms are compared and analyzed. The results show that when the load is added to 1.0kN, the deflections of the PV panels under two connections forms are less than the theoretical value of 16.82mm, meeting the normal use requirements; when the load is added to 2.1kN, the maximum strains of the PV panels are less than the limit strain 1712με, the PV panels are not failure. The PV plate has better bearing performance under the new "external form" connection form with smaller deflection and strain, which can be used as a new solution for the integration of PV construction.

1. Introduction

The concept of Building-integrated Photovoltaic (BIPV) was put forward by the World Energy Organization in 1986 [1]. Solar energy is cheap and abundant, which is beneficial to the energy consumption of buildings, and the combination of PV power generation system and building occupies no extra ground space. Accordingly, the integration of PV architecture is the future development trend of China.

Some researches on the mechanical properties of building-integrated PV roofing system have being carried out at home and abroad. Luo and Wu [2] summed up the characteristics and advantages of various application forms of PV steel structure integration system, and introduced the mechanical test model of PV modules. He [3] studied the dynamic performance of PV frame without substructure by numerical simulation. Wu [4] designed and developed an embedded module PV module and carried out the corresponding mechanical performance test. Yu et al. [5] measured the wind pressure on the typical roof PV panels and fitted the wind pressure coefficients numerically. Stathopoulos et al. [6] studied the distribution of wind pressure on the surface of PV panels on flat roofs. Zhang et al. [7] analyzed the wind load characteristics of PV panels. Warsido et al. [8] studied the influence of spacing parameters on the wind load of solar array.

At present, the studies on the mechanical properties of PV panels are not enough. In this paper, two new connection forms of PV panels and slope roofs have been designed and under which the

mechanical properties of PV panels also have been studied. The purpose is to get a more reasonable connection form to provide the potential for the engineering application of integrated PV architecture.

2. Optimal inclination design of PV panel

This paper has established a model of a villa facing the south in the Xuzhou area (figure 1) to study the optimal horizontal inclination of the PV receiving surface throughout the year. Using the current typical analysis software Autodesk Ecotect Analysis, the optimal horizontal inclination of the PV receiving surface is determined by its maximum annual total power generation [9]. The meteorological data for the Xuzhou area uses the China Standard Weather Data (CSWD) coming from the US Department of Energy Energy Efficiency and Renewable Energy website.

A 1.2m×0.54m plane model as the same size as the actual PV panel has been built on the villa roof facing the south, and the material is set as a solar collector in Autodesk Ecotect Analysis. The PV material in the parameters is crystal and the photoelectric conversion efficiency is 12% according to most practical conditions. Keeping the orientation unchanged, the PV panel model is rotated by the axis of its south side edge at inclinations of 0° to 90° to get annual total power generations under different inclinations. The data is shown in figure 2. The annual total power generation reaches a peak at 20° indicating that the optimal horizontal inclination is around 20°.

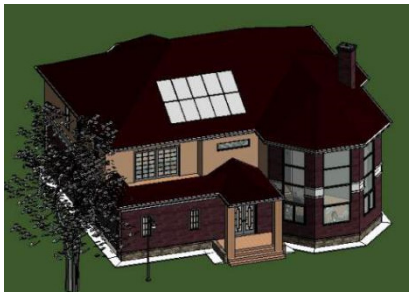

Figure 1. Villa model.

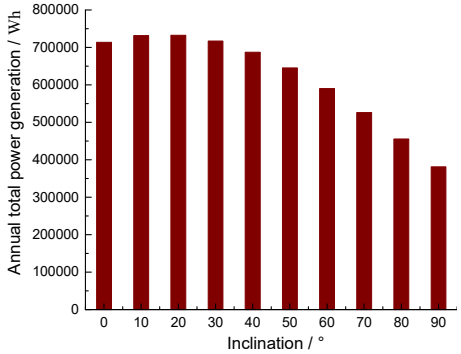

Figure 2. Different inclined PV plate model annual generating capacity histogram.

3. Calculation of test load and theoretical deflection

According to the "Load code for the design of building structures" GB 50009-2012, in addition to the self-weight effect, the roof also bears wind load, snow load, ash load and roof live load. The test load applied on the PV panel is the combination of live load, wind load, snow load and ash load. Their combined value coefficients ψ_c are taken as 0.7, 0.6, 0.7 and 0.9 respectively.

The standard values of roof live load and ash load are 0.5kN/m^2 according to the load code.

The standard value of wind load w_k is calculated as follows:

$$w_k = \beta_z \mu_s \mu_z w_0 \tag{1}$$

Where w_k is the standard value of wind load; β_z is the wind vibration coefficient; μ_s is the wind load shape coefficient; μ_z is the wind pressure height variation coefficient; w_0 is the basic wind pressure.

The standard value of snow load S_{snow} is calculated as follows:

$$S_{snow} = \mu_r \times S_0 \tag{2}$$

Where μ_r is the snow distribution coefficient of the house; S_0 is the basic snow pressure.

The external load combination value S is calculated as follows:

$$S = \gamma_{Q1} S_{Q1k} + \sum_{i=2}^{n} \gamma_{Qi} \psi_{ci} S_{Qik} \tag{3}$$

Where γ_{Qi} is the partial coefficient of the ith variable load; γ_{Q1} is the partial coefficient of the dominant variable load Q_1; ψ_{ci} is the combined value coefficient of the ith variable load Q_i; S_{Qik} is the load effect value calculated by the ith load standard value Q_{ik}; S_{Q1k} is the dominant load effect value.

The total external load F applied on the PV panel is calculated as follows:

$$F = S \cdot A \tag{4}$$

Where A is the area of the PV panel; S is the external load combination value as above.

The "Crystalline silicon terrestrial PV (PV) modules – Design qualification and type approval" (GB/T9535-2005)[10] provides that the PV panels should be able to bear load of 2400Pa. According to the "Manual of static Analysis for Building Structures", the maximum mid-span deflection f_{max} of the PV panel is calculated as follows:

$$f_{\max} = \frac{ql^4}{384EI} \tag{5}$$

Where q is the long-side equivalent line load of the PV panel; l is the length of the long side of the PV panel; E is the elastic modulus of the PV panel; I is the section inertia moment of the PV panel.

The value of F and f_{max} *are* calculated to be 1.0kN and 16.82mm.

4. Experimental design

4.1. The design of PV modules

There are two general connection forms: one is to place PV panels directly on the roof panels, described as “external form”; One is to integrate PV panels (as parts of the building structure) with roof panels in order to achieve interaction, described as “embedded form”.

Figure 3(a) is the “external form” designed in this paper. The I beam rails are arranged on the roof to make a certain gap between the PV panel and the roof surface to ventilate and dissipate heat to prevent the reduction of efficiency due to excessive temperature. The rails are connected to the roof beams by M8 bolts pre-buried on the roof panel (neglected in the figure). The PV panel is placed on the rails and its two ends are fixed by the connecting pieces. The load on the PV panel is transmitted to the rails and then transmitted to the roof beams. The connecting pieces are made of cold-formed thin-walled steel, 1mm thick. They are connected with the rails by the M6 bolts through two bolt holes reserved at both ends. The connecting piece detail is shown in figure 3(c). The rails adopt No.10 I beams, 100mm×68mm×4.5mm×7.6mm and the roof beams are made of 70mm×70mm square steel tubes with the thickness of 1mm. Figure 3(b) is the “embedded form” designed in this paper. The roof beam is made of No.5 channel steel, 50mm×37mm×4.5mm×7mm, and the PV panel is placed in it.

The PV panels adopted in the test are 1196mm×541mm×30mm in dimension and 7.8kg in weight. The surface of the PV panel is 3.2mm thick ultra white cloth tempered glass with high transmittance and strong bearing capacity. It is the main bearing member of the PV panel with the compressive strength of 125MPa and the elastic modulus of 73GPa.

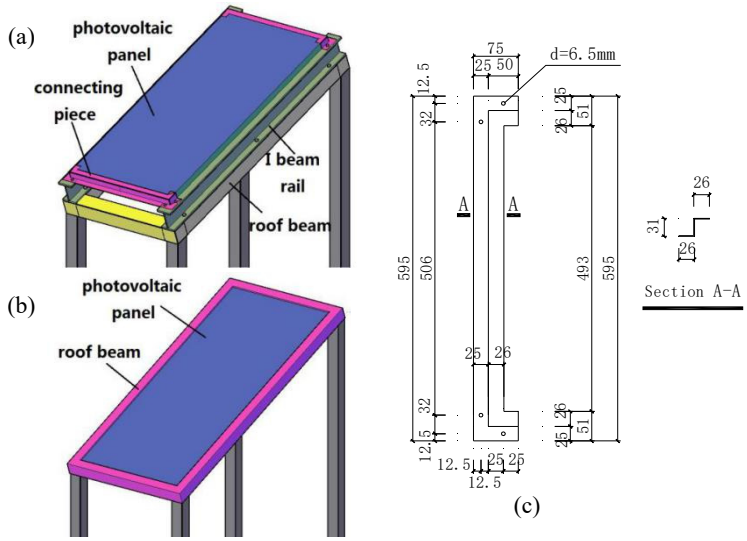

Figure 3. Designs of different connections between PV panel and slope roof: (a) external form, (b) embedded form, (c) connecting piece.

4.2. Test arrangement

The arrangements of PV modules are shown in figure 4. After assembly, the end of each module is welded on the channel steel fixed on the ground, and the two corners of the other end are respectively welded on steel piers fixed by ground anchors, so as to achieve the purpose of rigid connection between PV modules and substructure. There is a certain height difference between the steel piers and the channel steel to make the inclination of PV panels around 20 degrees.

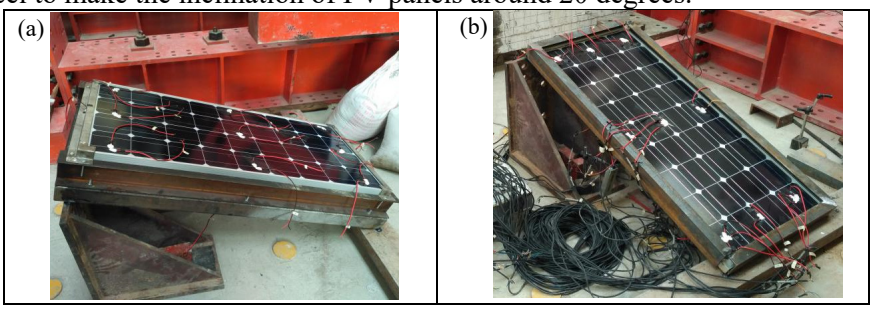

Figure 4. Test set-ups: (a) external form, (b) embedded form.

4.3. Loading method

The test is carried out under step loading by sand. Considering that the external load on the PV panel is 1.0kN in actual use and the manufacture data of its bearing capacity is 1.5kN, the test loading is 0.25kN at each step until adding to 1.5kN. Then change the step loading to 0.2kN until test loading can't be increased due to collapse of sand. It is 2.1kN. The test loading is shown in figure 5.

4.4. Measuring method

The arrangement diagrams of the strain gauges and deflection meters of the "external form" and "embedded form" are shown in figure 6. The strain gauges 28 and 29, 30 and 31, 32 and 33 of "external form" are attached to the mid-span of connecting pieces, upper flanges of I beam rails and square steel tubes respectively to measure the maximum strain of them. The strain gauges 28 to 31 of "embedded form" are attached to the mid-span of channel steels' lower flanges also to measure their maximum strains. 5 deflection meters (D1 to D5) are arranged both in the test of "external form" and "embedded form". The deflection meters D1 and D3 are arranged at the mid-span of square steel tubes

or channel steels, the others are arranged at the mid-span of short side and the quartering points of long side of PV panels to measure their deflections outside the plane respectively.

Figure 5. Test loading.

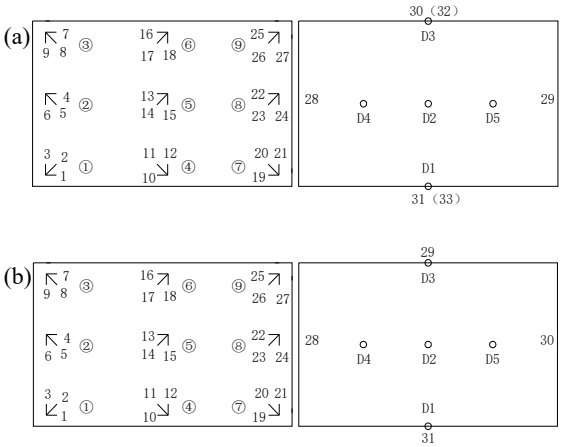

Figure 6. Strain and deflection gauges arrangement diagram: (a) external form, (b) embedded form.

5. Test data analysis

The maximum strain measured by strain rosettes at each point is calculated as follows:

$$\left.\begin{matrix}\varepsilon_{\max}\\ \varepsilon_{\min}\end{matrix}\right\}=\frac{\varepsilon_{0^\circ}+\varepsilon_{90^\circ}}{2}\pm\sqrt{\left(\frac{\varepsilon_{0^\circ}-\varepsilon_{90^\circ}}{2}\right)^2+\left(\frac{\varepsilon_{0^\circ}+\varepsilon_{90^\circ}-2\varepsilon_{45^\circ}}{2}\right)} \tag{6}$$

The maximum strain measured by strain rosette 1 (strain gauges 1, 2, 3) is recorded as strain 1, and so on. The strain values measured on connecting pieces, I beam rails, square steel tubes of "external form" and channel steels of "embedded form" are very small, indicating that the forces on them are small. The values measured by the deflection meters D1 and D3 are very small indicating that the deformations of square steel tubes and channel steels can be neglected. They are not analyzed.

5.1. Analysis of "external form"

Figure 7 and figure 8 are the load-strain curve and load-deflection curve of the "external form" PV panel. It can be seen from figure 7 and figure 8 that the strains and deflections of the PV panel are basically linear with the load during the loading to 2.1kN. The distribution of strains on the PV panel is symmetrical. The maximum strain and maximum deflection appear at the center of the panel, and the strain2, strain5 and strain8 in mid-spans are larger than the strains on both sides, which is consistent with the stress characteristics of the one-way slab (the short side of the PV panel is suspended). When the load is added to 1.0kN, the maximum deflection of the panel is 6.34mm, which is less than the theoretical value of 16.82mm. The PV panel meets the requirement of normal use. The ultimate strain of the PV panel tempered glass is calculated to be 1712με, and the maximum strain is much less than this value. There is no failure phenomenon on the PV panel.

5.2. Analysis of "embedded form"

Figure 9 and figure 10 are the load-strain curve and load-deflection curve of the "embedded form" PV panel. It can be seen from figure 9 and figure 10 that the strains and deflections of the PV panel are substantially linear with the load during the loading to 2.1kN. The distribution of strains on the PV panel is also symmetrical. The maximum strain and maximum deflection appear at the center of the panel. Since the four sides of the PV panel are placed in the channel steels, the strains in the four sides mid-spans are relatively larger consistent with the stress characteristics of the two-way slab. When the load is added to 1.0kN, the maximum deflection of the panel is 7.19mm, which is less than the

theoretical value of 16.82mm. The PV panel meets the requirements of normal use. The maximum strain is much less than the ultimate strain 1712με, there is no failure phenomenon on the PV panel.

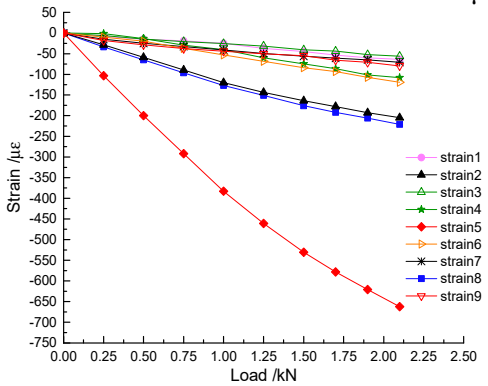

Figure 7. Load-strain curve of external form.

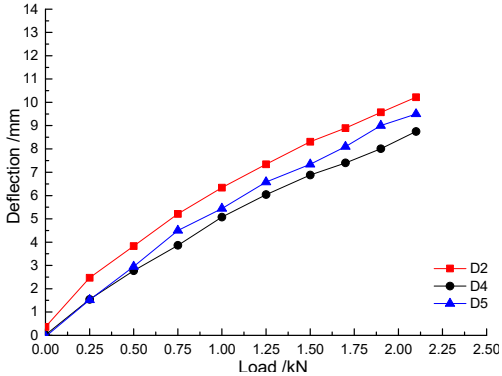

Figure 8. Load-deflection curve of external form.

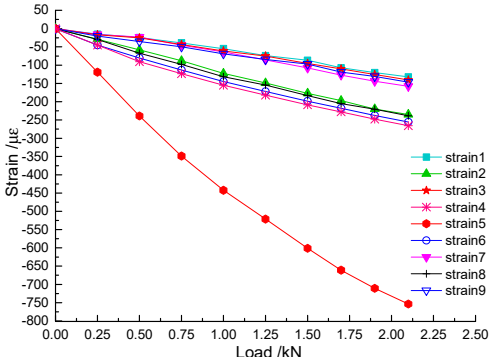

Figure 9. Load-strain curve of embedded form.

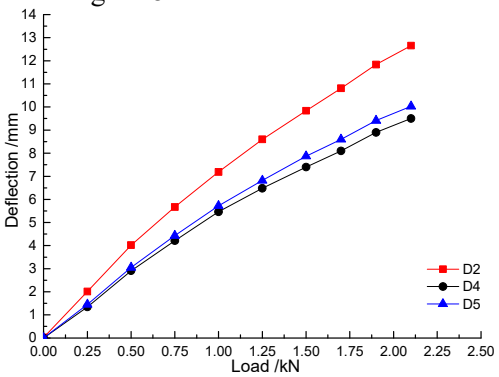

Figure 10. Load-deflection curve of embedded form.

5.3. Comparative analysis between "external form"and"embedded form"

Figure 11 is the load-strain comparison curve of two connection forms, and the maximum strains at the center of PV panels are selected for comparison. It can be seen from the figure that the maximum strain of the "external form" PV panel is smaller than that of the "embedded form" PV panel by 12% approximately. Figure 12 is the load-deflection comparison curve of the two connection forms. It can be seen from the figure that the deflection of each point of the "external form" PV panel is less than that of the "embedded form" PV panel, and the maximum deflection is smaller by about 19%.

According to the comparative analysis of strains and deflections, it can be concluded that the "external form" is more reasonable for the stress.

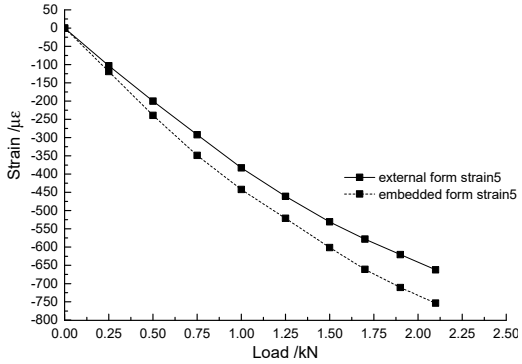

Figure 11. Load-strain comparison curve of two forms.

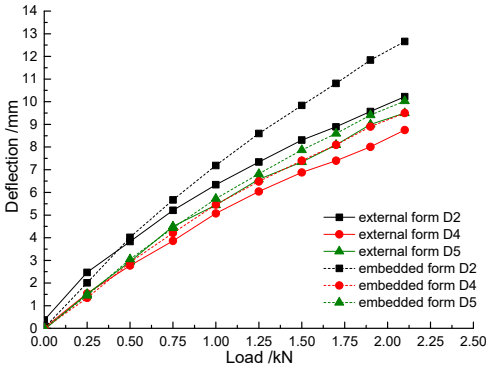

Figure 12. Load-deflection comparison curve of two forms.

6. Conclusion

In this paper, two new connection forms of PV panels and slope roofs have been designed, and static loading tests of the PV modules under them have been carried out. The conclusions are as follows:

(1) At the prophase of loading, the strains and deflections of PV panels are substantially linear with loads. The PV panels are in the elastic deformation stage. When the load is added to 1.0kN, the deflections of PV panels under the two connection forms are less than the theoretical value of 16.82mm, which satisfies the requirement for normal use;

(2) Under the test loading condition, the deflections of the PV panels increase with the load, but there is no failure phenomenon on the PV panels. The actual bearing capacity of the PV panel is much higher than the factory data;

(3) The strains and deflections of the connecting pieces, I beam rails, square steel tubes and channel steels are very small, indicating that the two connection forms are safe and reliable;

(4) Among the two connection forms, the PV panel has better mechanical behavior under the new "external form", and the maximum strain and maximum deflection are smaller than those of "embedded form" by 12% and 19% respectively. This connection form with simple structure is easy to construct, and is beneficial to the ventilation and heat dissipation of the PV panel to improve workability. It provides a new scheme for building integrated photovoltaic construction.

References

[1] Shi T, Shen J Y and Jing J Y 2011 *N. Build. Mater*. **38** 38-41
[2] Luo Y Z and Wu C W 2010 *Steel Constr.* **8** 44-48
[3] He J Dynamic analysis of photovoltaic modules and supporting structure 2013 *Zhejiang University of Technology*
[4] Wu C W Research of photovoltaic steel structure Integrated system and embedded modular PV module's research & design and application 2010 *Zhejiang University*
[5] Yu X L, Dong R and Wang S Q 2016 *J. Tongji Univ.* **44** 542-549
[6] Stathopoulos T, Zisis I and Xypnitou E 2014 *J. Wind Eng. Ind. Aerodyn*. **125** 195-206
[7] Zhang A S, Gao C L and Shen C J 2016 *Chin. J. Comput. Mech*. **33** 683-688
[8] Warsido W P, Bitsuamlak G T and Barata J 2014 *J. Fluids Struct.* **48** 295-315
[9] Wei Z D, Huo X P and He Y S 2012 *J. Xi'an Univ. Archit. Technol.* **44** 700-706
[10] GB/T 9535 2005 *Crystalline silicon terrestrial photovoltaic(PV) modules - Design qualification and type approval*